Article

Assessing the Development and Intensity of the Urban Heat Island through Weather Types in the Attica Region, Greece

Ilias Petrou [1], Nikolaos Kyriazis [1] and Pavlos Kassomenos [1]*

[1] Department of Physics, University of Ioannina, 45110, Greece, i.petrou@uoi.gr (I.P.), pph200771@uoi.gr (N.K.), pkassom@uoi.gr (P.K.)

* Correspondence: pkassom@uoi.gr

Abstract: In this study we investigated the association between weather types (WTs) and the Urban Heat Island Intensity (UHII) in the region of Attica (Greece). The application of the methodology results in ten WTs over Attica region. The UHII was calculated for every hour of the day from 2008 to 2017, using a new air temperature dataset produced by Copernicus Climate Change Service. To obtain more definitive findings about the relationship between WTs and UHII, we have used also the upper 5% of UHII (Urban Overheating-UO). The UO have been estimated for two-time intervals (daytime and nighttime) and for the warm period (June-September). The UHII frequency distribution as well as the spatial characteristics of the UO were also investigated. It was found that UO was amplified under WT2 during the night while, WT10 was mainly related with increased UO magnitudes at daytime, in all months. Furthermore, analysis results revealed that the UO effect is more pronounced in Athens during the night, especially at Athens center. The daytime hot-spots identified mainly in sub-urban and rural areas. Therefore, this methodology may help for heat mitigation strategies and climate adaptation measures, in urban environments.

Keywords: urban climate; Copernicus dataset; urban heat island; weather types; urban overheating; synoptic classification

1. Introduction

The expansion of built environment, as well as the extend of population and density of a city, causes substantial alterations in the usage and cover of land in metropolitan areas. Nowadays, it is well-established that these land cover changes, significantly influence local climate and weather conditions between a city and its rural surroundings [1,2]. However, there is a propensity to apply temperature as a measure that most clearly separates a city from the nearby countryside. A large body of the international literature has demonstrated that urban areas are, on average, warmer than their sub-urban and rural surroundings [3–6]. This effect, is referred to as the urban heat island (UHI). UHI is a local-scale, anthropogenically generated phenomenon. It is very complex as regards its dynamics, the space and time scales that operates. In general, the causes of UHI include the increase of heat capacity in cities, reduction of evaporation and evapotranspiration due to buildings materials, complex urban infrastructure, paved surfaces and reduced vegetation; the release of air pollutants in urban areas, associated with excess of heat trapped; the local morphological and surface geometry, the city's size, its population density and the local weather conditions [7].

The combination of high-speed urbanization processes, the increase of urban population and UHI effects, pose human health and well-being risk, especially for the elderly and other vulnerable groups (low-income citizens), who are frequently located in thermally vulnerable places [8]. The effects of the UHI including also changes in urban energy budget, social, economic and environmental issues [9,10]. Investigating synergies between UHI and heat waves in Athens, Founda and Santamouris (2017) found positive feedback between those factors, which may increase the thermal risk in cities [11].

Local meteorological phenomena, such as changes in precipitation rates, changes in frequency of lightning strokes and formation of clouds and fog, may be strongly affected by UHI [12,13]. Conversely, one of the key factors influencing the development and intensity of UHI is the local weather conditions. In this context, vumerous studies have been undertaken, in order to find influences of singular climate variables on the magnitude of the UHI. For instance, Ngarambe et al. (2021) found increased UHI intensities (UHII) under low wind speeds, clear skies and densely built areas in Seoul [14]. On the other hand, in Thessaloniki (Greece), Giannaros and Melas (2012) concluded that UHI decreases with increasing wind speed [15]. In Pearl River Delta area (east China), Wang et al. (2015) examined the UHI and meteorological elements and indicated that the UHI intensity decreases with increasing low cloud cover, relative humidity, wind speed and precipitation [16]. Additionally, in Sydney (Australia) the presence of a sea breeze in the eastern sections of the city was associated with high UHI intensities [17].

Since, the focus of much urban overheating (UO) research is on the interaction of UHI with individual meteorological variables (wind speed, temperature, relative humidity, cloud cover, etc.), the association between UHI intensities/patterns and large-scale prevailing weather conditions in a given location, are largely absent from such univariate approaches. It is also necessary to have a deeper understanding of how synoptic-scale meteorological conditions affect the spatial and temporal patterns of UO since these variables will affect local-scale conditions in urban areas. In this context, weather type categorizations have proven very useful tools in such researches. Among others, in Lisbon's Metropolitan Area, rainy days and sunny days (especially very cold winter days) were linked with lower and higher median UHI intensities, respectively [18]. Moreover, during daytime UO is associated with humid, humid warm and warm conditions in Athens and Thessaloniki (Greece), and with warm, humid warm, dry and dry warm conditions during nighttime [6]. In Sydney, Khan et al. (2021) utilizing the gridded weather typing classification (GWTC2), found that high UO magnitudes, were related with humid warm and warm air-masses, during extreme heat events and in all seasons [19].

However, the majority of existent studies on associations between UO and synoptic weather conditions evaluated the UHI effects by using already developed weather typing classification and one (or more) urban and rural stations, in order to calculate temperature differences between urban and rural places. In this study, a definition of weather types (WTs) for the 41-year period (1980–2020) was conducted, by applying statistical methods on the recently released high-resolution grid point meteorological data over the Mediterranean and Attica region (Greece). In addition, high temporal resolution and good spatial resolution data, from Copernicus dataset, were applied in order to investigate UHII and examine the influence of WTs which were defined, on UO magnitude in Attica region.

2. Materials and Methods

2.1. Study area

The undertaken research is focused in geographical region of Attica in Greece, that encompasses the entire Athens Metropolitan area, the country's capital and largest city. Attica is a highly crowded, built-up region that lacks open spaces and green areas, and covers about 3,808 km^2. The permanent population increased to 3.8 million inhabitants in 2011 with a density of 1250 inhabitants/km^2, while more than 95% are inhabitants of the Athens metropolitan area (Hellenic Statistical Authority; https://www.statistics.gr/statistics/pop). In addition, Attica region is a triangular peninsula jutting into the Aegean Sea and is watered by gulfs of the Aegean Sea. In the center of the peninsula, there is a large basin where the entire metroplex of Athens-Piraeus has been constructed. This basin is surrounded by four mountains: Hymettus, Parnitha (the highest mountain of Attica), Egaleo and Penteli (Figure S1), providing significant amounts of green. According to the Hellenic National Meteorological Service (HNMS), Attica is one of the warmest regions in Greece with mean monthly temperatures and precipitation heights range from 8.8 ^{o}C to 28.3 ^{o}C and from 1.6mm to 12.5mm, respectively (http://www.emy.gr/emy/en/climatology/climatology).

Preprints (www.preprints.org) | NOT PEER-REVIEWED | Posted: 26 May 2023 doi:10.20944/preprints202305.1871.v1

2.2. Meteorological data

For the purpose of this study, two sets of data were obtained from the NCEP/NCAR Reanalysis (https:// iridl. ldeo. colum bia. edu/ SOURC ES/. NOAA/. NCEPNCAR/. CDAS- 1/. DAILY/), covering a 41-year time period (1980–2020) [20]. Since the NCEP/NCAR database is the longest reanalysis database and uses the full set of available observations, it was chosen above other existing datasets. The first set of data contains 2.5° x 2.5° intrinsic daily grid point values of 500 and 1,000 hPa geopotential heights, 850 hPa temperature and 850 hPa specific humidity over the main geographical domain of the Mediterranean region (30°N–45°N, 10°E–35°E) (Figure 1). The second set comprises daily diagnostic gridded meteorological variables at 1° x 1° (2 m temperature, specific humidity, 2m zonal and meridional wind, total cloud cover, precipitation rate and convective precipitation rate) for the geographical domain of central Greece (37°N–39°N, 22.5°E–24.375°E), including the region of Attica (Figure 1). The geopotential heights data describe the atmospheric circulation conditions over the region, whereas the above meteorological parameters that we used provide crucial information on the meteorological and climatic conditions prevailing over the Attica region [21].

Figure 1. The study's geographic areas were the Mediterranean region (wider domain, on the left) and the Attica region (sub-domain, on the right).

2.3. Copernicus urban climate dataset

To achieve a detailed spatial distribution of the UHI in the Attica region, we used the dataset presented by the Copernicus Climate Change Service [22]. This dataset contains hourly gridded values (air temperature, specific humidity, relative humidity and wind speed) for 100 European cities and from 2008 to 2017, with a spatial resolution of 100m. The data were produced using the UrbClim urban climate model. This model was created with a geographical resolution of 100 m (at the scale of a city neighborhood) to simulate and research the UHI and other urban climatic factors, and requires two types of input data: large-scale meteorological data (downscaling of ERA 5 reanalysis) and terrain data (land use, vegetation, and soil sealing).

Therefore, in this study hourly air temperature gridded data at the height of 2m above the surface, were obtained in NetCDF-4 format for Athens between 2008 and 2017. June, July, August, and September were only selected, representing summer season. The temperature data were divided into daytime (06:00–18:00 LT) and nighttime (23:00–06:00 LT), to explore the UHI effects in day ($\Delta T_{daytime}$) and night ($\Delta T_{nighttime}$) for Athens. Land-sea mask and rural-urban mask data were also obtained to isolate land area form sea area and separate urban from rural area.

 doi:10.20944/preprints202305.1871.v1

2.4. Formation of the prevailing WTs

In the present study, in order to identify the WTs over the Attica region, we employed a combination of two main statistical methods; k-means cluster analysis (CA) and components analysis (PCA). In climatology, both statistical methods are often employed [23–25].

PCA is a dimensionality-reduction technique that is frequently used to decrease the dimensionality of big data sets. It does this by splitting a large number of variables (X_1+X_2..., X_i) into a smaller set of variables called "principal components" (PCs), which are formed in such a way that they are uncorrelated [26]. In PCA, rotation of the factor axes (dimensions) is a method that rotates the eigenvectors (factors) in an effort to produce a simple structure [27]. Rotation methods are either orthogonal (equamax, orthomax, quartimax and varimax) or oblique. Orthogonal rotation methods assume that the factors in the analysis are uncorrelated. The varimax rotation was utilized in this study, which is the most common orthogonal rotation method that that maximizes high- and low-value factor loadings and minimizes mid-value factor loadings. The optimal number of PCs is indicated by the SCREE plot graph along with the physical meaning of the PCs. The eigenvalues are shown on the SCREE plot as a descending slope, ranging from greatest to lowest [28].

A set of variables with similar properties are grouped together into objectively defined groupings (clusters) using the statistical approach known as cluster analysis (CA). In exploratory data analysis, CA is frequently employed because it can reveal patterns or relationships in the data that might not be immediately apparent [29]. For cluster analysis, a variety of techniques are employed, including k-means, hierarchical clustering, and density-based clustering. In the present study, the non-hierarchical method k-means was utilized to find clusters while the Euclidean distance was used to assess case similarity. Additionally, by employing the distortion test, which is based on the typical distance between observations and cluster centers, the ideal number of clusters were indicated [30].

As the first stage of the particular approach utilized here, PCA is applied on the correlation matrix including the two sets of variables. More specifically, the first matrix includes 500 and 1,000 hPa geopotential heights, 850 hPa temperature and 850 hPa specific humidity over the wider domain of the Mediterranean region and the second matrix contains the meteorological values over sub-domain, namely 2m temperature, specific humidity, 2m zonal component and meridional component wind, total cloud cover, precipitation rate and convective precipitation rate. In order to group the days into clusters with homogenous climatic features, the K-means CA algorithm was applied in the second step to the set of PCs that were retained. On this basis, local WTs could be located and our findings could be directly compared to those of other research carried out in the same area.

2.5. UHI intensity calculation

The difference in temperature between urban and rural regions at a given time is known as UHI intensity (UHII) [31,32]. The non-urban points must be located outside of the built-up urban region or any surface that has been altered by constructions (asphalt, cement, etc.), since this site has traditionally been linked with a rural area. Hence, the UHII was calculated for every hour of the day from 2008 to 2017 according to the following equation:

$$\mathbf{\Delta Ti} = T_{urb} - T_{rul\ (mean)} \quad (1)$$

where ΔTi represent the UHII, T_{urb} is the 2 m temperature for each urban grid point and $T_{rur\ (mean)}$ is the 2m temperature averaged over the rural grid points. The ΔTi frequency distribution at daytime and nighttime for each month was also examined. Additionally, in order to find associations between local WTs and urban overheating (UO), and have more clear view of these associations, we have used also the higher 5% of daily maximum ΔTi for both daytime and nighttime.

However, the city's bounds are frequently erroneous since the urban continuum occasionally lacks distinct boundaries, suggesting a shift toward normally rural land usage [33]. In our case, the rural area is represented by the rural classes of CORINE (coordination of information on the environment) covering grassland, cropland, shrubland, woodland, broadleaf forest and needleleaf forest (https://land.copernicus.eu/pan-european/corine-land-cover). More specifically, according to the land-sea mask, land area receives value 1 and is represented by the land classes of CORINE, sea

Preprints (www.preprints.org) | NOT PEER-REVIEWED | Posted: 26 May 2023 doi:10.20944/preprints202305.1871.v1

area receives missing value NaN and is represented by the sea classes of CORINE, while according to the rural-urban mask, rural area receives value 1 and is represented by the rural classes of CORINE, urban area receives missing value NaN and is represented by the urban classes of CORINE.

3. Results and discussion

3.1. Definition of WTs over the 41-year time period (1980-2020)

The application of PCA on the two data sets of the wider domain and the sub-domain, and for the entire 41-year time period, resulted in 5 PCs in each case (representing 88.1% and 77.3% of the total variance, respectively). The number of PCs was based on the results of the SCREE plots (Figure S2), as has already mentioned above. The application of CA on all the 10 resultant PCs together, leads to 10 distinct and homogeneous clusters according to the distortion test (Figure S3). Considering that each of the 10 clusters defines a specific WT. Table 1 displays the average values of the meteorological variables for each of the 10 WTs. The WTs frequency was also investigated in Attica region from 1980 to 2020 (Figure 2). WT2 and WT 10 were the most frequent WTs in all seasons (average around 19% of the time), followed by WT1 (12%), WT8 (11%), WT4 (11%), WT9 (8%), WT7 (7.2%), WT6 (5.3%), WT3 (4.1%) and WT5 (3%).

Table 1. Mean values for each WT's associated weather variables.

WTs	Specific humidity	Temperature (ºC)	u wind (m/sec)	v wind (m/sec)	Cloud cover (%)	Wind direction (º)
WT1	0.0083	15.0	3.3	-0.2	32.9	W
WT2	0.0119	23.8	-0.4	-2.3	20.4	N
WT3	0.0075	10.8	-1.9	-5.2	58.1	NNE
WT4	0.0066	11.1	-1.3	-2.3	24.9	NNE
WT5	0.0106	15.9	-0.2	3.2	69.0	S
WT6	0.0082	12.7	3.4	2.9	51.1	SW
WT7	0.0078	12.7	-4.1	-1.5	56.0	ENE
WT8	0.0093	16.4	0.0	3.1	54.4	S
WT9	0.0058	8.9	-0.7	-4.1	24.9	N
WT10	0.0113	23.9	0.3	-1.6	16.4	N

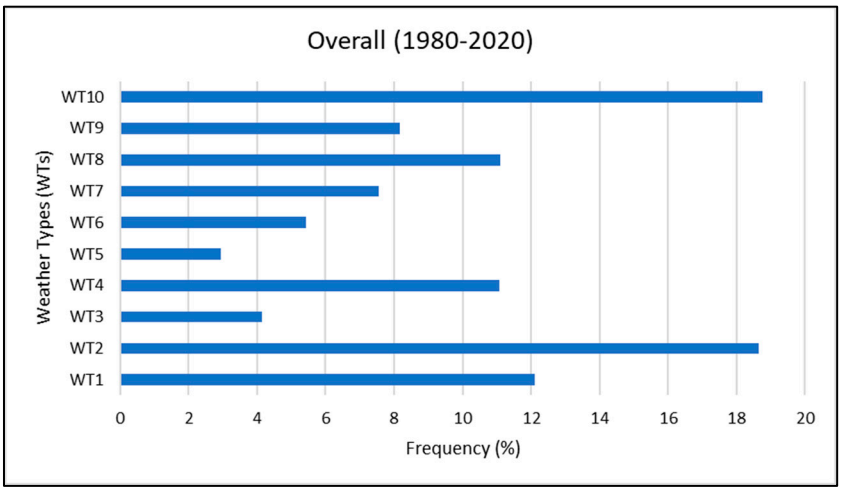

Figure 2. Overall WTs frequency for Attica region from 1980 to 2020.

 doi:10.20944/preprints202305.1871.v1

The 41-year period's long-term average patterns of 1,000 hPa geopotential height for each WT, are displayed in Figure 3. WT2 and WT10 are typically warm period WTs, due to the fact that mainly prevail between May and September, and their frequency present a maximum at August and July respectively (Figure 3). The Azores high-pressure system over southern Europe and the expansion of the Asiatic Low into the eastern Mediterranean are both responsible for these characteristic summer circulations. These atmospheric patterns are also responsible for the formation of the Etesian winds (northerly direction) over the Aegean Sea [34,35]. More specifically, WT10 present its maximum frequency in July and associated with high temperatures, partly cloudy conditions and limited precipitation. The weak pressure gradient over Aegean causing low wind speeds mainly from northerly directions. According to Kassomenos and Katsoulis (2006), these atmospheric situation favors the formation of local circulations such as sea breezes, carrying humid air masses from the sea [36]. On the contrary, the maximum of WT2 frequency appears in August, where the Etesian winds outbreaks are most frequent [37], and associated with stronger northerly flow. Air temperature is high and cloud cover and precipitation is generally low, while according to Lolis and Kotsias (2020), this WT is generally dry [21].

WT3, WT4 and WT9 are cold period WTs, correlate to low-pressure systems across the southeast Mediterranean, centered on the southeast Aegean Sea, and Cyprus (Figure 3). During the winter, these atmospheric circulation patterns are typical and associated with low temperatures, cloud development (Table 1) and rainy weather conditions over the Aegean Sea [38]. They prevail between October to May, causing a northeasterly flow over the southern Balkans, and transfer cold air masses from eastern Europe, and can be related with prolonged sunshine in North Greece [39].

WT5, WT6, WT7 and WT8 are also cold WTs, generally prevails from October to May. These WTs corresponding to low-pressure systems over the Ionian Sea, whilst anticyclonic conditions are present in the north-eastern Balkans (Figure 3), cause S-SW flow over the southern Balkans, and in case of WT7 ENE flow. These types of circulations are associated with low temperatures and extensive cloud cover (Table 1) that can be followed by precipitation events [40], especially over the western part of the country [41].

WT1 could be considered also as a cold period WT, prevails mainly from November to May, with a depression over the North East Balkans and over Middle East, and an anticyclone over the central Mediterranean (Figure 3). The temperature is relatively low and cloud cover characterized but low values (Table 1). Such atmospheric circulation causes westerly air flow and associated with dry weather conditions and low precipitation [39].

Preprints (www.preprints.org) | NOT PEER-REVIEWED | Posted: 26 May 2023 doi:10.20944/preprints202305.1871.v1

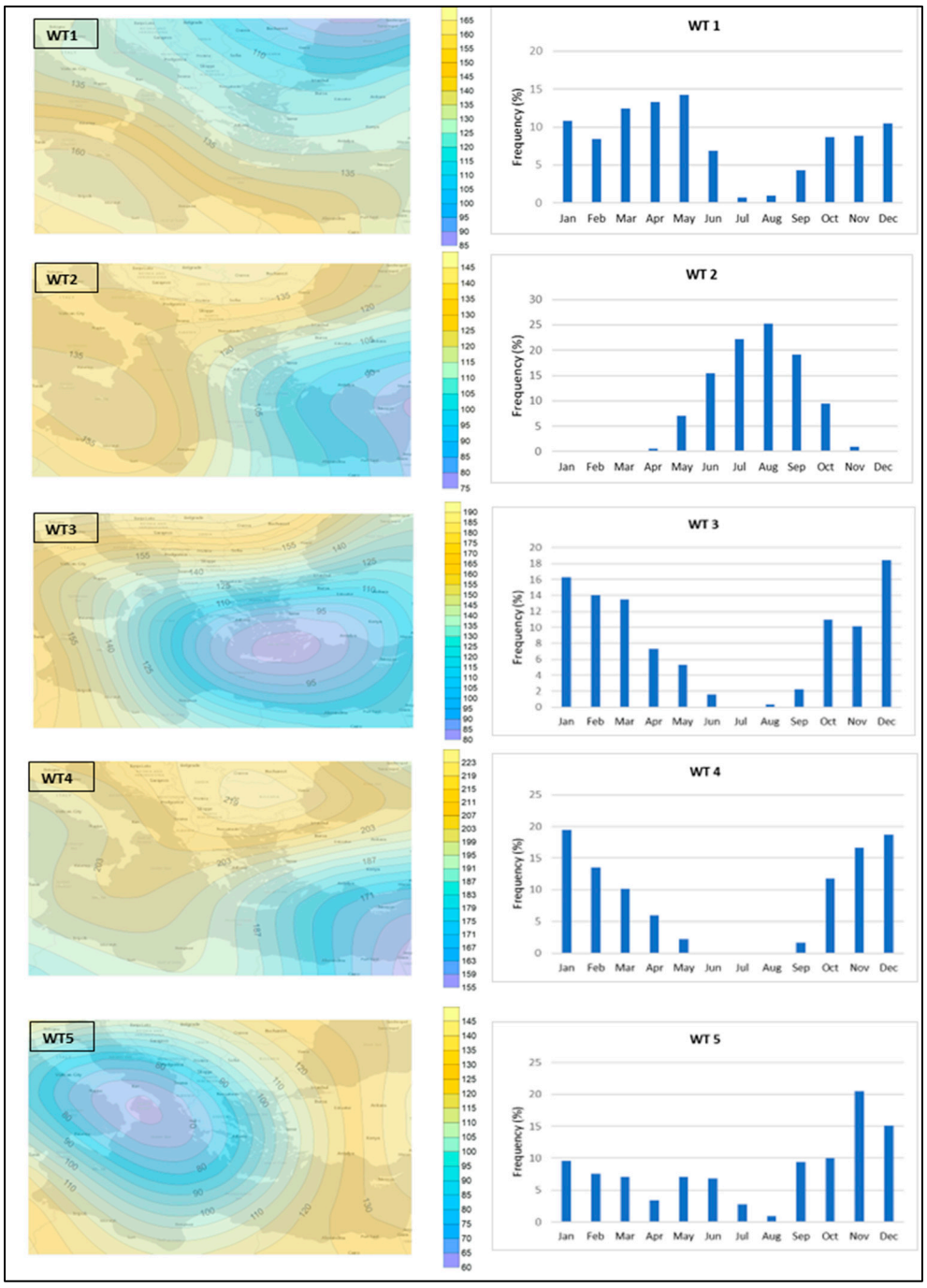

Preprints (www.preprints.org) | NOT PEER-REVIEWED | Posted: 26 May 2023 doi:10.20944/preprints202305.1871.v1

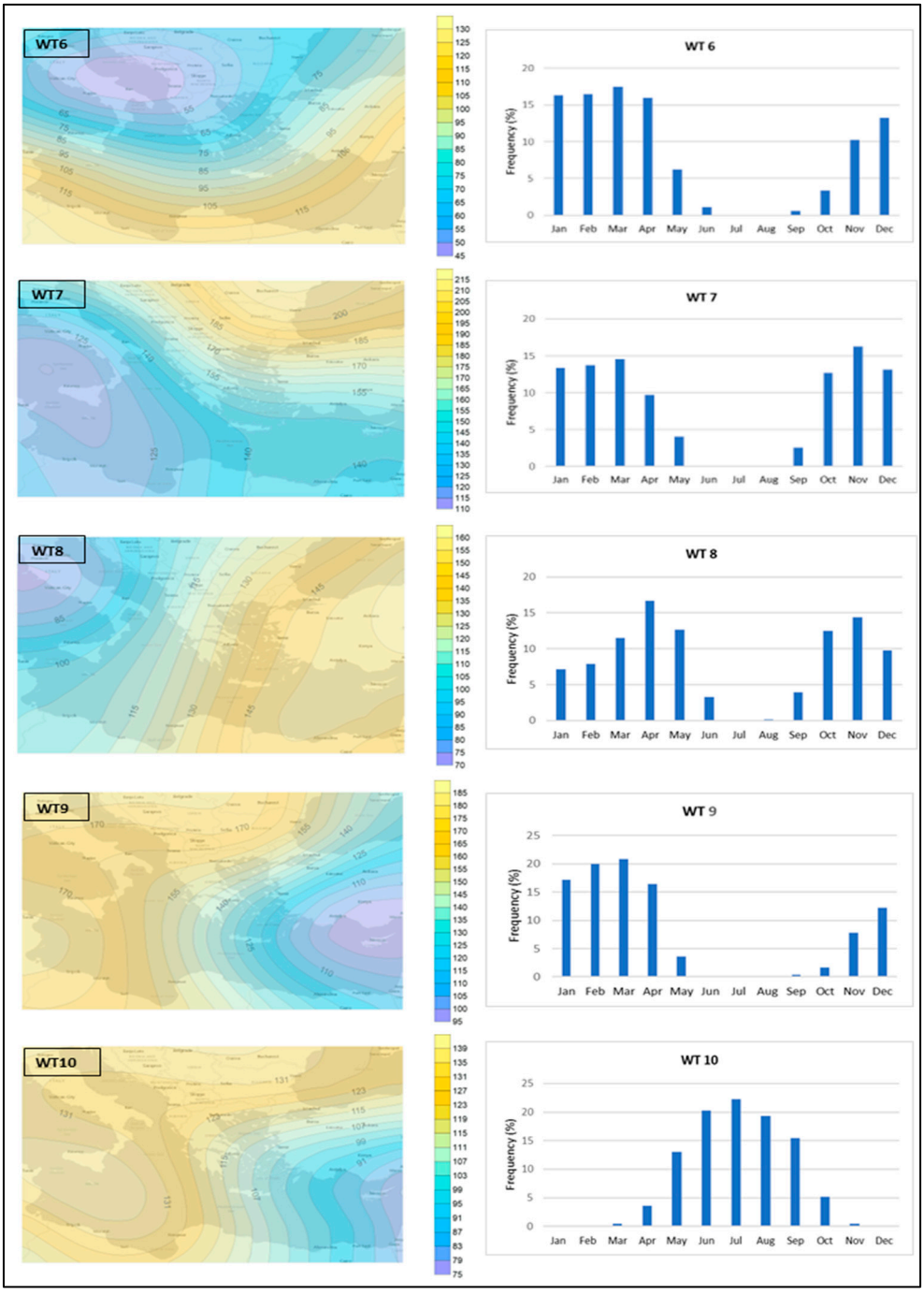

Figure 3. The long term means patterns of 1000 hPa geopotential height (gpm) and the annual frequency variation of the 10 WTs.

3.2. UHI intensity frequency distribution

Suburban-urban temperature difference (ΔTi) frequency distribution throughout the day and at night was examined for all months during the summer, from 2008 to 2017 (Figure 4). As it was mentioned above, the ΔTi represent the UHII in Attica region. In June, the daytime ΔTi was reported positive for about 53%, while negative appeared for 40%. As for the nighttime in June, ΔTi appeared positive for 58% and negative for 31%. In July, the daytime and nighttime ΔTi calculated positive for about 62%, in contrast to the negative daytime and nighttime ΔTi which reached a percentage close to 28%. In August, the daytime ΔTi was reported positive for 52% and negative for 32%. Contrarily, during the August night ΔTi was found positive for 62% and negative for only 27%. Finally, in

Preprints (www.preprints.org) | NOT PEER-REVIEWED | Posted: 26 May 2023 doi:10.20944/preprints202305.1871.v1

September the daytime ΔTi was observed positive for 46% and negative for 40%, while the nighttime ΔTi was positive for 60% and negative for 31%.

Comparing the frequency distribution, the higher frequencies of positive ΔTi observed during the night, especially in July and August (62%). Moreover, in all cases the positives ΔTi outweigh the negatives ΔTi, while in August observed the highest difference between positive and negatives ΔTi (62% against 27%, at nighttime).

It is evident that UHI is more pronounced during the night than the day, in agreement with previous studies of UHI formation, who found that UHI is primarily a nocturnal phenomenon, due to the fact that in the late afternoon and evening, urban areas fail to cool as quickly as the surrounding rural regions [4,18]. Similarly, previous studies for Athens reported that the highest UHII are related mostly during the nighttime hours [42,43]. For instance, Giannaros et al., (2013) who studied the UHI over Athens by using WRF model, found significantly higher nighttime temperatures for the Athens metropolitan area compared to the nearby non-urbanized areas [44]. The surface of the city serves as an urban heat sink throughout the day, while during the night, the city's surface seems to be warmer than its surrounds, as noted by Keramitsoglou et al., 2011 [45].

Figure 4. UHII frequency distribution for each month in Attica region at daytime and nighttime.

 doi:10.20944/preprints202305.1871.v1

3.3. Association of WTs with UO magnitudes

To assess the relationship between the daily WTs and the UO in summer, the upper 5% of daily daytime and nighttime maximum ΔTi (UO) was calculated. Figure 5 depicts the higher 5% of maximum ΔTi (UO) at Attica region for summer, under different weather types. It is apparent that WT2 and WT10 are the only weather conditions in daytime, enhancing the UO magnitude. More specifically, WT10 contributed for about 52.4% and WT2 for 47.6% of the time. The median value of the UO magnitude in daytime during WT10 was estimated equal to 7.4 °C, comparatively higher during WT2 conditions (6.9 °C).

While examining the association between UO magnitude and WTs in nighttime, it was observed that UO is associated with more than two WTs. As it illustrated in Figure 5, WT2, WT10, WT8, WT6, WT5 and WT1, related with UO during the night in summer. However, WT2 and WT10 are the most dominant weather conditions. In terms of WTs frequency, during the night WT10 contributed for 44.8% and WT2 for 50.9% of the time, followed by WT8 (1.7%), WT5 (1.5%), WT6 (0.6%) and WT1 (0.3%). Furthermore, estimates of the median value of the UO magnitude during the night were found equal to 8 °C for WT2 and 8.1°C for WT10, slightly higher compared to those in daytime. It appears that daytime UO was amplified under WT10, while during the night UO associated mainly with WT2.

These results do not come as a surprise, as the WT2 and WT10 are typical summer circulations and the most frequent WTs in all seasons. According to Kassomenos et al. (2022), the warm WTs were more frequently documented in Athens, notably in recent years and during summertime, and the highest urban overheating levels were correlated with warm and humid conditions during the day and dry warm conditions at night [6]. Additionally, Kassomenos and Katsoulis (2006), have stated that high UHI classes in Athens associated with similar conditions as those of WT2 and WT10 (a combination of the Azores Anticyclone and SW Asia thermal low) [36]. Similarly, Mihalakakou et al., (2002), studied the impact of synoptic-scale atmospheric circulation on the UHI over Athens and identified anticyclonic synoptic category characterized by weak flow regime, favors the development of UHI phenomenon [46].

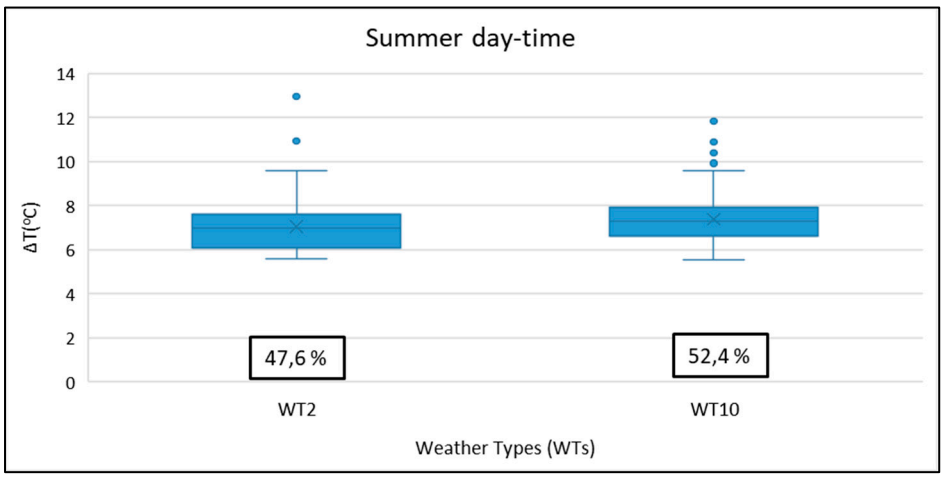

Preprints (www.preprints.org) | NOT PEER-REVIEWED | Posted: 26 May 2023 doi:10.20944/preprints202305.1871.v1

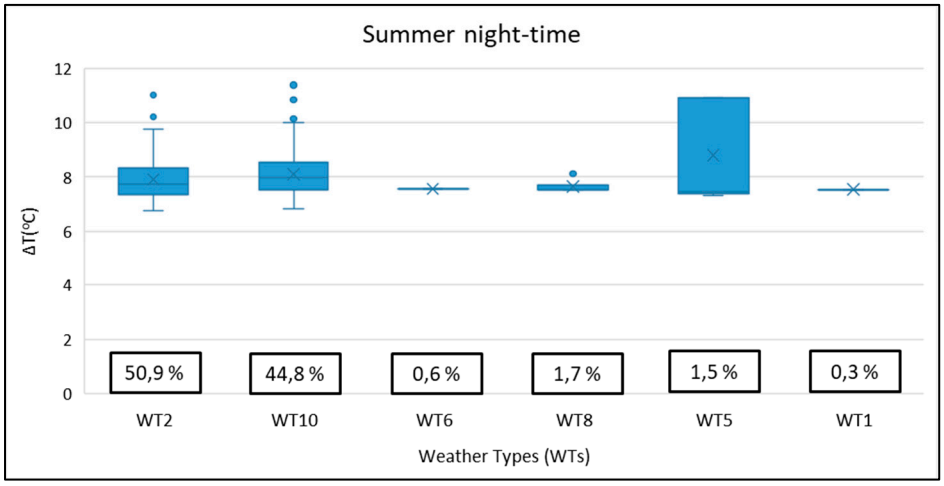

Figure 5. The upper 5% of the daytime daily maximum ΔT (°C) and nighttime daily maximum ΔT (°C) in summer, under different WTs, at Attica region.

3.4. Spatial characteristics of the UO during summer

The spatial characteristics of mean UO values illustrated in Figure 6, for each month during the summer (daytime and nighttime), from 2008 to 2017. It is apparent that, in June, during the day the UO extends to the whole Athens metropolitan area, including the Athens urban area (also known as Greater Athens), Piraeus, northwest suburban areas and rural areas of East Attica. The UO magnitude at these sites varied between 8 and 11 °C on average. During the night in June, the UO mainly limited to the Athens urban area, Piraeus and some suburban areas in southeast Attica. In case of July, UO hot-spots (8 -11 °C) found mainly near suburban areas mount Hymettus at East Attica, at north near Mount Penteli (Mesogeia), at west near Mount Parnitha and Mount Egaleo (Petroupoli and Nikaia). During night hours in July, UO highest magnitudes related with the central municipalities of the Athens Greater Area (City of Athens, Piraeus, Moshaton, Kallithea, N. Smyrni). Remarkable is the reduction in terms of UO magnitudes, during the day in August. The daytime hot-spots are located mainly at west of Athens urban area (Egaleo), while nighttime hot-spots in August appeared at the central municipalities of the Athens Greater Area. Similar patterns were observed in September, although during the night UO hot-spots are expand also to the east suburban and rural areas (Mesogeia).

For all cases, during the daytime, hot-spots located mainly in suburban and rural areas, such as Egaleo and Mesogeia, reaching their maxima in June and September. On the other hand, a thorough examination during the night in Figure 6, reveals that nighttime UO hot-spots related with urban areas, including the Athens center and central municipalities of the Athens Greater Area. As for UO magnitudes, nighttime hot-spots exhibited similar behavior, reaching their maximum values in early/later summer. These findings support those of Giannaros et al. (2013) who found the existence of three daytime hot-spots, at Megara, Elefsina and Mesogeia, while in the nighttime, the city centre is modeled to be warmer than its surroundings [44]. Furthermore, this behavior is well known for Athens, as already reported in Keramitsoglou et al., (2011) [45]. The combined impact of the topography and surface cover features determines the UO hot-spots of Athens throughout the day. For instance, Mount Hymettus is to the east of Mesogeia, which is bordered to the north by Mount Penteli's slopes, including areas with sparse low vegetation, such as olive trees and vineyards, industrial zones as well as areas covered with bare soil, such as the Athens International Airport "El. Venizelos''. Such semi-rural environments start heating very fast at daytime and cooling quickly after sunset due to its open exposure and its low thermal surface materials. Conversely, the higher release of stored heat from urban surfaces like concrete and asphalt causes the cooling rate of the densely populated urban environment to be greatly lowered. It is worth mentioning that, high surface temperatures during heat waves, may reduce the definition of these hotspots.

Preprints (www.preprints.org) | NOT PEER-REVIEWED | Posted: 26 May 2023 doi:10.20944/preprints202305.1871.v1

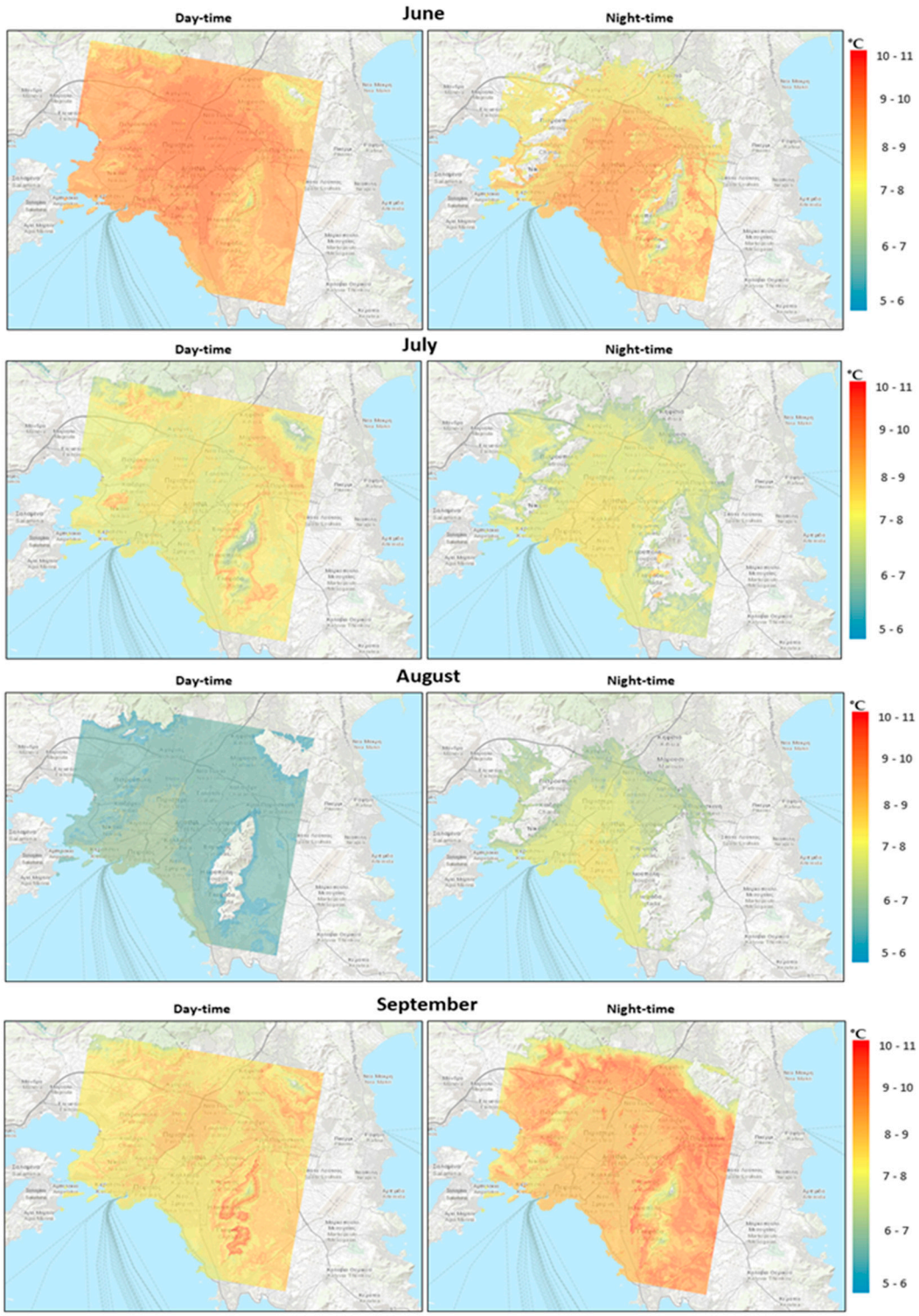

Figure 6. Spatial variation of the UO for each month in daytime and nighttime.

4. Conclusions

In the present study, a classification of WTs was conducted and implemented, for studying the UHI effect over the Attica region (Greece) during the summer, for both day and night. An association between UO and daily WTs conditions, as well as the spatial characteristics of the UO were also investigated. For this purpose, a brand-new, publicly accessible dataset on urban climate from Copernicus Climate Change Service was used. The analysis above allowed for the following conclusions to be formed:

1. The warm period WTs, (WT2 and WT10) were reported to occur with a higher frequency, between 1980 to 2020.
2. As previous studies have shown, UHII in Attica region was found exacerbating during the night, suggesting that UHI is mainly a nighttime phenomenon.
3. WT10 was mainly responsible for exacerbated UO magnitude at daytime in all months, while UO at nighttime was mostly attributed to WT2 conditions.
4. WT10 is associated with the weak pressure gradient over Aegean causing low wind speeds mainly from northerly directions, in contrast with WT2 which is associated with stronger northerly flow.
5. During the day, high UO magnitudes occur mainly in sub-urban and rural areas (Mesogeia, Penteli, Aspropyrgos) of Attica region. Conversely, UO hot-spots consistently located in urban areas, including the Athens center and central municipalities of the Athens Greater Area. In both cases, the UO reaching their maxima in June and September.

These findings highlight that, studying the UHI effect under the influence of different atmospheric circulation patterns, provide essential information on the prevention and control of the negative UO effects in a densely populated city like Athens. UHI effects become even more important when considering that in a changing climate, the frequency of warm weather types will increase with their frequency [47]. Future researches, however, would benefit from extending the investigation to the winter and looking at how UHI differs depending on the weather throughout all aspects of its daily cycle. These findings can also be applied by the local government and the public health for heat mitigation techniques and climate adaption methods in metropolitan areas.

Author Contributions: Conceptualization, P.K and I.P..; methodology, I.P. and N.K.; formal analysis, K.P. and I.P.; writing—original draft preparation, I.P.; writing—review and editing, I.P and P.K..; supervision, P.K. All authors have read and agreed to the published version of the manuscript.

Funding: This research received no external funding.

Data Availability Statement: The authors do not have permission to share the data.

Conflicts of Interest: The authors declare no conflict of interest.

References

1. Mohammad Harmay, N.S.; Kim, D.; Choi, M.; Urban Heat Island associated with Land Use/Land Cover and climate variations in Melbourne, Australia, *Sustainable Cities and Society*, **2021**, Volume 69, 102861.
2. Kim, J. P.; Guldmann, J. M. Land Use Planning and the Urban Heat Island. *Environment and Planning B Planning and Design*. **2014**, 41. 10.1068/b130091p.
3. Sismanidis, P.; Keramitsoglou, I.; Kiranoudis, C.T. A satellite-based system for continuous monitoring of surface urban Heat Islands. *Urban Clim*. **2015**, 14, 141–153. http://dx.doi.org/10.1016/j.uclim.2015.06.001.
4. Oke, T.R.; Mills, G.; Christen, A.; Voogt, J.A. Urban climates. *Cambridge University Press*. **2017**, https://doi.org/10.1017/9781139016476.
5. Santamouris, M. Heat Island Research in Europe: The State of the Art. *Advances in Building Energy Research*, **2007,** 1:1, 123-150, DOI: 10.1080/17512549.2007.9687272
6. Kassomenos, P.; Kissas, G.; Petrou, I.; Begou, P.; Khan, H.S.; Santamouris, M. The influence of daily weather types on the development and intensity of the urban heat island in two Mediterranean coastal metropolises, *Science of The Total Environment*, **2022**, Volume 819, 153071, https://doi.org/10.1016/j.scitotenv.2022.153071.
7. Oke, T. R.; Johnson, G. T.; Steyn, D. G.; Watson, I. D. Simulation of surface urban heat islands under ideal conditions at night part 2: Diagnosis of causation. *Boundary-Layer Meteorol*., **1991**, 56, 339–358.
8. Heaviside, C.; Vardoulakis, S.; Cai, X.M. Attribution of mortality to the urban heat island during heatwaves in the West Midlands, UK. *Environ. Health,* **2016**, 15. http://dx.doi. org/10.1186/s12940-016-0100-9.
9. Oliveira, A.; Lopes, A.; Niza, S.; Soares, A. An urban energy balance-guided machine learning approach for synthetic nocturnal surface Urban Heat Island prediction: A heatwave event in Naples, *Science of The Total Environment*, **2022**, Volume 805, 150130, https://doi.org/10.1016/j.scitotenv.2021.150130
10. Tang, J.; Di, L.; Xiao, J.; Lu, D.; Zhou, Y. Impacts of land use and socioeconomic patterns on urban heat Island, *International Journal of Remote Sensing*, **2017**, 38:11, 3445-3465, DOI: 10.1080/01431161.2017.1295485

11. Founda, D.; Santamouris, M. Synergies between Urban Heat Island and Heat Waves in Athens (Greece), during an extremely hot summer. *Sci Rep*, **2017**, 7, 10973. https://doi.org/10.1038/s41598-017-11407-6
12. Orville, R.E.; Huffines, G.; Nielsen-Gammon, J.; Zhang, R., et al. Enhancement of cloud to-ground lighting over HoustonTexas. *Geophysical Research Letters*, **2001**, 28, 2597–2600.
13. Shem, W.; Shepherd, M. On the impact of urbanization of summertime thunderstorms in Atlanta: two numerical model case studies. *Atmos. Res*, **2009**, 92, 172–189.
14. Ngarambe, J.; Oh, J.W.; Su, M.A.; Santamouris, M.; Yun, G.Y. Influences of wind speed, sky conditions, land use and land cover characteristics on the magnitude of the urban heat island in Seoul: an exploratory analysis. *Sustain. Cities Soc*., **2021**, 71, 102953.
15. Giannaros, T.M.; Melas, D. Study of the urban heat island in a coastal Mediterranean City: the case study of Thessaloniki, Greece. *Atmos. Res*., **2012**, 118, 103–120. https://doi.org/10.1016/j.atmosres.2012.06.006.
16. Wang, B.; Ding, S.; Qiao, G.; Guo Y.; Wu Y. Study on the Urban Heat Islands and the Meteorological Elements over the Pearl River Delta. *ICUC9 - 9th International Conference on Urban Climate jointly with 12th Symposium on the Urban Environment*, **2015.**
17. Santamouris, M.; Haddad, S.; Fiorito, F.; Osmond, P.; Ding, L.; Prasad, D.; Zhai, X.; Wang, R. Urban Heat Island and overheating characteristics in Sydney. Australia. An analysis of multiyear measurements. *Sustainability*, **2017**, 9 (5), 712
18. Reis, C.; Lopes, A.; Nouri, S.A. Assessing urban heat island effects through local weather types in Lisbon's Metropolitan Area using big data from the Copernicus service, *Urban Climate*, **2022**, Volume 43, 101168, https://doi.org/10.1016/j.uclim.2022.101168.
19. Khan, H.S.; Santamouris, M.; Kassomenos, P.; Paolini, R.; Caccetta, P.; Petrou, I. Spatiotemporal variation in urban overheating magnitude and its association with synoptic airmasses in a coastal city. *Sci. Rep*., **2021**, 11, 6762.
20. Kistler, R.; Kalnay, E.; Collins, W.; Saha, S.; White, G.; Woollen, J.; Chelliah, M.; Ebisuzaki,W.; Kanamitsu, M.; Kousky, V.; Van DenDool, H.; Jenne, R.; Fiorino, M. The NCEP–NCAR50-year reanalysis: monthly means CD-ROM and documentation. *Bulletin of the American Meteorological Society*, **2001**, 82(2), 247–267.
21. Lolis C.J.; Kotsias, G. The use of weather types in the definition of seasons: the case of southern Balkans. *Theor Appl Climatol* , **2020**, 142:1199–1219. https:// doi. org/ 10. 1007/ s00704- 020- 03369-z
22. Hooyberghs, H.; Berckmans, J.; Lefebre, F.; De Ridder, K. C3S_422_Lot2 SIS European health. UrbClim extra documentation 1–18. **2019**, Available on. https://cds. climate.copernicus.eu/cdsapp#!/dataset/sis-urban-climate-cities?tab=form.
23. Borge, R.; Lumbreras, J.; Vardoulakis, S.; Kassomenos, P.; Rodriguez, E. Analysis of long–range transport influences on urban PM10 using two–stage atmospheric trajectory clusters. *Atmos Environ*, **2007**, 41:4434–4450
24. Mohammed, A.J.; Alarcón, M.; Pino, D. Extreme temperature events on the Iberian Peninsula: statistical trajectory analysis and synoptic patterns. *Int J Climatol*, **2018**, 38(14):5305–5322
25. Markou, M.T.; Kassomenos, P. Cluster analysis of five years of back trajectories arriving in Athens, Greece. *Atmos Res*, **2010**, 98 (2– 4):438–457. https:// doi. org/ 10. 1016/j. atmos res. 2010. 08. 006
26. Jolliffe, I.T. Principal component analysis. *Springer*, New York, **1986**.
27. Bryant, F.B.; Yarnold, P.R. Principal-components analysis and exploratory and confirmatory factor analysis. In L. G. Grimm & P. R. Yarnold (Eds.), Reading and understanding multivariate statistics. *American Psychological Association*, **2015**, (pp. 99–136).
28. Bartzokas, A.; Metaxas, D.A. Factor analysis of some climatological elements in Athens, 1931-1992: covariability and climatic change. *Theor Appl Climatol*, **1995**, 52(3–4):195–205
29. Sharma, S. Applied Multivariate Techniques. New York, **1995**, ISBN:978-0471310648: John Wiley & Sons 512 pp.
30. Sugar, C.A.; James, G.M. Finding the number of clusters in a dataset. *Journal of the American Statistical Association*, **2003**, 98 (463), 750–763. https://doi.org/10.1198/016214503000000666
31. Alcoforado, M.J.; Lopes, A.; Alves, E.D.L.; Can´ario, P. Lisbon heat island statistical study (2004-2012). *Finisterra,* **2014**, 49 (98), 61–80. https://doi.org/10.18055/Finis6456.
32. Oke, T.R.; Mills, G.; Christen, A.; Voogt, J.A. Urban climates. *Cambridge University Press*, **2017,** https://doi.org/10.1017/9781139016476
33. Martin-Vide, J.; Sarricolea, P.; Moreno-García, M.C. On the definition of urban heat island intensity: the "rural" reference. Front. *Earth Sci*., **2015**, 3, 24. https://doi.org/10.3389/feart.2015.00024.

34. Anagnostopoulou, C.; Zanis, P.; Katragkou, E.; Tegoulias, I.; Tolika, K. Recent past and future patterns of the etesian winds based on regional scale climate model simulations. *Clim Dyn*., **2014**, 42(7–8):1819–1836.
35. Paschalidou, A.K.; Kassomenos, P.A. What are the most fire-dangerous atmospheric circulations in the Eastern-Mediterranean? Analysis of the synoptic wildfire climatology. *Sci Total Environ*, **2016**, 539:536–545.
36. Kassomenos, P.; Katsoulis, B. Mesoscale and macroscale aspects of the morning Urban Heat Island around Athens, Greece. *Meteorol. Atmos. Phys*., **2006**, 94, 209–218. https://doi.org/10.1007/s00703-006-0191-x
37. Tyrlis, E.; Lelieveld, J. Climatology and dynamics of the summer etesian winds over the eastern Mediterranean. *Journal of the Atmospheric Sciences*, **2013**, 70(11), 3374–3396. https://doi.org/10.1175/jas-d-13-035.1.
38. Houssos, E.E.; Lolis, C.J.; Bartzokas, A. Atmospheric circulation patterns associated with extreme precipitation amounts in Greece. *Adv Geosci*., **2008**, 17:5–11
39. Michailidou, C.; Maheras, P.; Arseni-Papadimititriou, A.; Kolyva-Machera, F.; Anagnostopoulou, C. A study of weather types at Athens and Thessaloniki and their relationship to circulation types for the cold-wet period, part I: two-step cluster analysis. *Theor App Climatol*., **2009**, 97(1–2):163–177.
40. Maheras, P.; Anagnostopoulou, C. In: Bolle HJ (ed) Circulation types and their influence on the interannual variability and precipitation changes in Greece. Mediterranean climate — variability and trends. *Springer Verlag*, Berlin, **2003**, pp 215–239.
41. Lolis, C.J. High-resolution precipitation over the southern Balkans. *Clim Res*. **2012**, 55:167–179
42. Dandou, A.; Tombrou, M.; Akylas, E.; Soulakellis, N.; Bossioli, E. Development and evaluation of an urban parameterization scheme in the Penn State/NCAR Mesoscale Model (MM5). *Journal of Geophysical Research*, **2005**, 110, D10102
43. Martilli, A.; Roulet, Y.A.; Junier, M.; Kirchner, F.; Rotach, M.W.; Clappier, A. On the impact of urban surface exchange parameterizations on air quality simulations: the Athens case. *Atmospheric Environment*, **2003**, 37, 4217e4231.
44. Giannaros, T.M.; Melas, D.; Daglis, I. A.; Keramitsoglou, I.; Kourtidis, K. Numerical study of the urban heat island over Athens (Greece) with the WRF model, *Atmospheric Environment*, **2013**, Volume 73, Pages 103-111, ISSN 1352-2310, https://doi.org/10.1016/j.atmosenv.2013.02.055.
45. Keramitsoglou, I.; Kiranoudis, C.T.; Ceriola, G.; Weng, Q.; Rajasekar, U. Identification and analysis of urban surface temperature patterns in Greater Athens, Greece, using MODIS imagery. *Remote Sensing of Environment*, **2011**, 115, 3080e3090.
46. Mihalakakou, G.; Flocas, H.A.; Santamouris, M.; Helmis, C.G. Application of neural networks to the simulation of the heat island over Athens, Greece, using synoptic types as a predictor. *J Appl Meteorol*, **2002**, 41: 519–527.
47. Petrou, I.; Kassomenos, P.; Lee, C. C. (2022). Trends in air mass frequencies across Europe. *Theoretical and Applied Climatology*, **2022**, 148(1–2), 1–16. https://doi.org/10.1007/s00704-022-03921-z